A Novel Diterpene Suppresses CWR22Rv1 Tumor Growth *In vivo* through Antiproliferation and Proapoptosis

Feng-Min Lin,[1] Chin-Hsien Tsai,[1] Yu-Chih Yang,[1] Wei-Chun Tu,[1] Li-Ru Chen,[1] Yun-Sa Liang,[1] Sheng-Yang Wang,[3] Lie-Fen Shyur,[1] Shih-Chang Chien,[1] Tai-Lung Cha,[2] and Pei-Wen Hsiao[1]

[1]Agricultural Biotechnology Research Center, Academia Sinica; [2]Division of Urology, Department of Surgery, Tri-Service General Hospital, National Defense Medical Center, Taipei, Taiwan and [3]Department of Forestry, National Chung-Hsing University, Taichung, Taiwan

Abstract

Androgen receptor (AR) is the main therapeutic target for treatment of metastatic prostate cancers (PCa). As recurrent tumors restore AR activity independent of hormones, new therapies that abolish AR activity have been sought to prevent or delay the emergence of ablation-resistant disease. Here, we report that a novel abietane diterpene, 6-hydroxy-5,6-dehydrosugiol (HDHS), isolated from the stem bark of *Cryptomeria japonica*, was a potent AR antagonist in PCa cells. HDHS treatment of androgen-dependent LNCaP and androgen-responsive 22Rv1 cells induced apoptosis as shown by nucleosome release, activation of caspase-3 and caspase-7, and cleavage of poly(ADP-ribose) polymerase accompanied with concomitant up-regulation of tumor suppressor p53. HDHS also decreased the protein expression of cyclins (D1 and E), cyclin-dependent kinases (CDK2, CDK4, and CDK6), and retinoblastoma phosphorylation in PCa cells, which suggest cell cycle arrest in the G_1 phase. Oral administration of HDHS at 0.5 and 2.5 mg/kg once daily for 24 days to 22Rv1 PCa xenografted mice suppressed tumor growth by 22% and 39%, respectively, in association with decreased proliferation and increased apoptosis in tumor cells, which further correlated with increased levels of HDHS in plasma and tumors. Overall, our data suggest that HDHS has potential for use in chemoprevention and chemotherapy of PCa. [Cancer Res 2008; 68(16):6634–42]

Introduction

Carcinoma of the prostate gland is the most common malignancy in males in the Western world (1) and is also one of the top 10 fatal cancers in Taiwan. Although the great majority of prostate cancers (PCa) initially respond to androgen ablation, recurrent tumors arise that become resistant, and at the terminal stage, patients succumb to widespread metastases (2, 3). Androgens execute their functions through binding to the androgen receptor (AR) that then regulates gene transcription in the cell nucleus. Androgen-AR activity is tightly associated with the growth, differentiation, and even carcinogenesis of the prostate (4, 5). In fact, expression of AR protein is detected in nearly all PCa, including those of distant metastases and ablation-resistant cases (6). AR also up-regulates the gene transcription of prostate-specific antigen (PSA), which is the most widely used serologic biomarker of PCa for both diagnosis and therapeutic assessment (7, 8). Previously, we exploited the PSA promoter, stably integrated in the chromatin of PCa 22Rv1 cells, as a target and searched for signaling inhibitors against PCa (9, 10).

Deregulation of the cell cycle contributes to the unrestrained proliferation in human cancer (11). Anticancer agents often modulate signal transduction pathways that regulate the cell cycle and result in cytostatic and even apoptotic effects. The eukaryotic cell cycle is controlled by interconnected biochemical events that coordinate the transition of cells from one phase to another (12). A series of molecular events in the G_1 phase must complete before the launch of chromosome replication in the S phase. During G_1 progression, cyclin D complexes with cyclin-dependent kinases (CDK), CDK4 and CDK6, to engender an active kinase complex that phosphorylates a variety of cellular substrates, the most well characterized being the tumor suppressor retinoblastoma (Rb), which is the gatekeeper for entry into the S phase (12, 13). Cyclin E forms a complex with CDK2 to further phosphorylate Rb with the release of general transcription factor E2F-1, which then stimulates the transcription of genes involved in DNA replication (13, 14). In addition to Rb, another important tumor suppressor required for maintenance of the G_1 checkpoint controls of the cell cycle is p53, a transcription factor whose half-life increases on activation (12, 13, 15). During apoptosis, a cascade of different caspases is cleaved and activated for the cleavage of critical cellular substrates, including poly(ADP-ribose) polymerase (PARP), whose cleavage activates the DNA repair enzyme (16, 17). Therefore, ideal chemopreventive or chemotherapeutic approaches often influence expression of the regulatory molecules of cell cycle progression and apoptosis.

Plant species contain scores of secondary metabolites. Research interest in the specific bioactivity and potential applications of plant compounds is increasing rapidly. Recently, we isolated some abietane diterpenes that suppress AR activity in PCa cells by novel mechanisms from *Cryptomeria japonica* D. Don (Taxodiaceae), also called Sugi or Japanese cedar (10). 6-Hydroxy-5,6-dehydrosugiol (HDHS) in particular (Fig. 1*A, inset*) exerted strong AR inhibitory activity and decreased cell growth in a cell type–specific manner. This study was designed to study the molecular mechanisms whereby HDHS negatively affected AR function as well as growth of human PCa *in vitro* and *in vivo*. HDHS inhibited AR through the ligand-binding domain (LBD) and induced AR nuclear localization. HDHS suppressed PCa growth by inducing apoptosis and blocked cell cycle progression during the G_1 phase of AR-dependent cells. Moreover, orally administered HDHS retarded CWR22Rv1 tumor growth in athymic nude mice without obvious toxic side effects and reduced proliferation and promoted apoptosis dose dependently in the tumors.

Note: Supplementary data for this article are available at Cancer Research Online (http://cancerres.aacrjournals.org/).

Requests for reprints: Pei-Wen Hsiao, Agricultural Biotechnology Research Center, Academia Sinica, 128 Academia Road, Sec. 2, Nankang, Taipei 115, Taiwan. Phone: 886-2-2651-5747; Fax: 886-2-2785-9360; E-mail: pwhsiao@gate.sinica.edu.tw.

doi:10.1158/0008-5472.CAN-08-0635

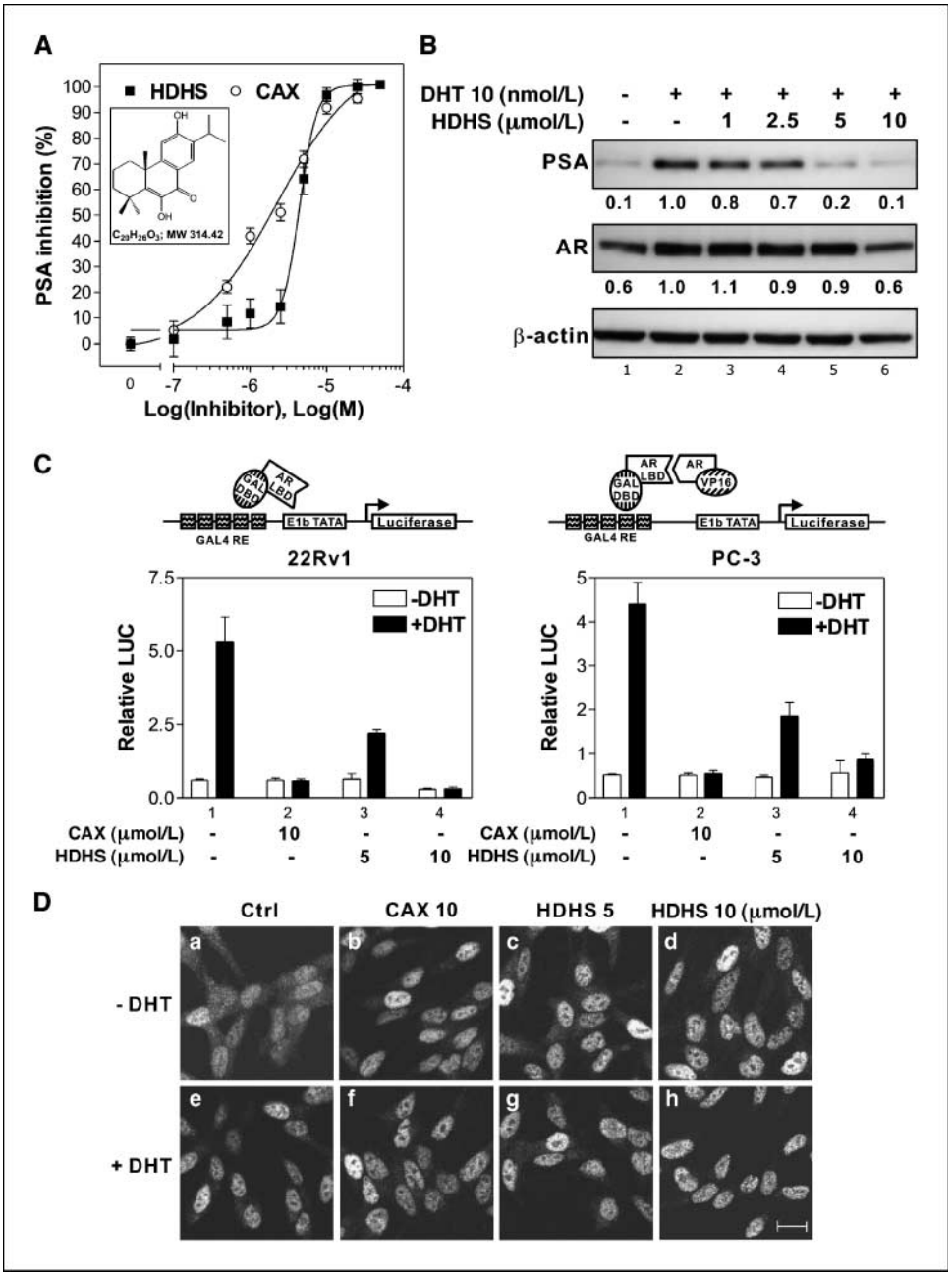

Figure 1. Effects of HDHS on AR in PCa cells. *A,* dose-response curves of HDHS and Casodex (*CAX*) in inhibiting DHT-induced PSA-luciferase reporter. 103E cells were grown and cotreated with 10 nmol/L DHT and indicated concentrations of HDHS and Casodex for 24 h. The PSA-Luc activities of treated cells were detected and inhibition of AR activity was analyzed. *Points,* mean of three independent experiments of three replicates; *bars,* SD. *Inset,* chemical structure and molecular formula of HDHS. *B,* LNCaP cells were treated with vehicle (*Ctrl*) or indicated concentrations of HDHS in the presence of 10 nmol/L DHT for 24 h. PSA and AR expression in tested cells (40 μg whole-cell lysate) was examined by Western blot with anti-PSA and anti-AR antibodies. Protein levels (relative to actin; listed below the first two blots) were quantitatively analyzed with Chemigenius^2 (Biolabo). The blots shown are representative of three independent experiments. *C,* one-hybrid and two-hybrid assays. *Left,* 22Rv1 cells were cotransfected with pG5E1b-Luc, pRL-CMV, and pCMX-GBD-AR(DE) for 24 h. The cells were then treated with Casodex or HDHS in the presence or absence of 10 nmol/L DHT for another 20 h. Luciferase activity in cell lysates was analyzed as described in Materials and Methods. *Right,* PC-3 cells were cotransfected with pG5E1b-Luc, pRL-CMV, pCMX-GBD-AR(DE), and pCMV-VP16AR(38-918) for 24 h. The cells were then treated with Casodex or HDHS as marked for 20 h. *D,* LNCaP cells were treated with vehicle, indicated concentrations of Casodex, or HDHS in the presence or absence of DHT for 1 h. The cellular AR was detected by immunofluorescent confocal microscopy. *Bar,* 20 μm.

Materials and Methods

6-Hydroxy-5,6-dehydrosugiol. 6,12-Dihydroxy-5,8,11,13-abietatetraen-7-one (Fig. 1*A, inset*) was isolated from the stem bark of *Cryptomeria japonica* as reported previously (10). HDHS was dissolved in DMSO (100 mmol/L) and then serially diluted with absolute ethanol into the 1,000× stock solutions of working concentrations. In cell-based assays, cell culture medium was refreshed with medium containing 0.1% (v/v) of HDHS stock solutions. In animal experiments, mice were dosed by force feeding with 200 μL HDHS (freshly diluted from 2 and 10 mmol/L of stocks with PBS into 10 volumes) to attain dosages of 0.5 and 2.5 mg/kg.

Chemical reagents and antibodies. Commercial chemicals and solvents were 5α-dihydrotestosterone (DHT), puromycin, and propidium iodide (Sigma-Aldrich); Casodex (Toronto Research Chemicals); and RNase (Amresco). DMSO, ethanol, *n*-hexane, methanol, and acetonitrile (J. T. Baker) were of analytic reagent or high-performance liquid chromatography (HPLC) grade. Antibodies to AR (N-20), cyclin D1 (C-20), cyclin E (M-20), CDK2 (M-2), CDK4 (H-22), CDK6 (C-21), Rb (C-15), p27 (F-8), p21 (F-5), p53 (DO1), Bcl-xL, and β-actin were purchased from Santa Cruz Biotechnology. Caspase-3 and caspase-7 antibodies were purchased from NeoMarkers/Lab Vision Corp. and Oncogene Research Products, respectively. PSA antibodies were purchased from Chemicon and PARP and phosphorylated Rb (Ser^{780}) antibodies were purchased from Cell Signaling.

Cell culture. LNCaP, PC-3, and 22Rv1 PCa cell lines were obtained from the American Type Culture Collection. Normal fibroblast NIH-3T3 cells were kindly provided by Dr. Lie-Fen Shyur. The 103E cell line was derived from 22Rv1 and contained a stably transfected PSA promoter luciferase reporter, which is expressed in an androgen-dependent manner as previously

described (9, 10). LNCaP, 22Rv1, and 103E cells were cultured in RPMI 1640 (Invitrogen) supplemented with 10% fetal bovine serum (FBS; Hyclone). PC-3 and NIH-3T3 were cultured in DMEM (Hyclone) supplemented with 10% FBS. Cultures were maintained in a humidified incubator at 37°C in 5% CO_2/air.

Cell viability and colony formation analyses. Equivalent 1×10^4 cells of PCa or NIH-3T3 lines were seeded into 96-well microtiter plates with 10% FBS culture medium. After 24 h, cells were incubated in 10% FBS medium containing different concentrations of HDHS or equivalent amounts of vehicle alone as control for 48 h. 3-(4,5-Dimethylthiazol-2-yl)-2,5-diphenyltetrazolium bromide (MTT) assay was performed with AlamarBlue (Serotec). Colony-forming cell growth was analyzed as described previously (9).

Transient transfection and luciferase assays. In one-hybrid assay, 22Rv1 cells (8×10^4 per well in 48-well plates) were cotransfected for 24 h with plasmids including pG5E1b-Luc (200 ng), pRL-CMV (50 ng), and pCMX-GBD-AR(DE) (175 ng) using Lipofectamine 2000 transfection reagent (Invitrogen). In mammalian two-hybrid assay, PC-3 cells (1.5×10^4 per well in 48-well plates) were cotransfected with plasmids including pG5E1b-Luc (200 ng), pRL-CMV (50 ng), pCMX-GBD-AR(DE) (175 ng), and pCMV-VP16AR(38-918) (75 ng). The transfected cells were treated with vehicle or various compound treatments for another 20 h. Luciferase activity was measured using luciferase reporter gene assay system (Promega) and normalized against respective *Renilla* luciferase values (18).

Immunofluorescence. LNCaP cells were grown in medium containing 5% charcoal-dextran–stripped FBS on 12-mm coverslips for 48 h and then treated with vehicle or various compound treatments for another 1 h. Cells were fixed with 4% (v/v) paraformaldehyde on ice for 15 min, permeabilized with 0.2% (v/v) Triton X-100/PBS, and then washed with PBS thrice. After blocking in 1% (v/v) fish gelatin/PBST (PBS with 0.1% Tween 20) for 1 h, samples were incubated with AR (C-19, Santa Cruz Biotechnology) antibody at 4°C for 18 h, washed thrice with PBST, and then probed with the respective fluorescence-conjugated secondary antibody (Alexa Fluor 488, Invitrogen) for 1 h at room temperature. The samples were washed again and mounted in mounting medium (Vector). The cellular location of AR was visualized by confocal microscopy (LSM 510 Meta, Carl Zeiss GmbH) and analyzed using the manufacturer's software.

Cell cycle analysis. The cell cycle of treated cells was examined by flow cytometry after cellular staining with propidium iodide. Cells (5×10^5) were seeded into six-well multidishes with 10% FBS culture medium for 48 h. Cells were treated with HDHS, Casodex, or vehicle for 48 h. Cells were trypsinized thereafter, washed twice with cold PBS, and centrifuged. The pellet was suspended in cold PBS and 1 mL of 70% ethanol at 4°C overnight, washed twice with cold PBS, and digested with RNase (100 μg/mL final concentration) and stained with propidium iodide (10 μg/mL final concentration) for 30 min and analyzed by flow cytometer (EPICS XL-MCL, Beckman Coulter, Inc.).

***In vivo* studies.** Athymic (*nu/nu*) nude mice (6–7 wk of age) were obtained from the National Laboratory Animal Center and housed in the Laboratory Animal Center of the National Defense Medical Center (Taipei, Taiwan) under conditions of constant photoperiod (12-h light/12-h dark) and fed with Laboratory Autoclavable Rodent Diet 5010 (LabDiet). All animal work was done in accordance with the protocol approved by the Institutional Animal Care and Use Committee, Academia Sinica. Aliquots of 1×10^6 22Rv1 cells were suspended in 1:1 PBS mixed with Matrigel (BD Biosciences) and were s.c. inoculated into the right flank of each mouse. After 1 wk, mice were stochastically assigned to three groups ($n = 7$) that received vehicle control or HDHS at different dosages (0.5 and 2.5 mg/kg/d), by gavage in 0.2 mL of PBS containing 10% DMSO. Tumors were measured twice weekly using calipers and their volumes were calculated using a standard formula as follows: width^2 × length × 0.5. Body weight was measured weekly. Mice received 24 doses, and 24 h after the last dose, they were sacrificed to harvest plasma and tumors. A portion of each tumor was snap frozen in liquid nitrogen and stored at −80°C until needed for Western blot analysis of relevant biomarkers, and the remainder was fixed in 10% formalin overnight.

Immunohistochemistry. The paraffin-embedded tumor sections (4 μm thickness) were heat immobilized and deparaffinized using xylene and rehydrated in a graded series of ethanol with a final wash in distilled water. Antigen retrieval was done in Target Retrieval Solution (DakoCytomation) in a Decloaking Chamber (Biocare Medical) followed by quenching of endogenous peroxidase activity. Sections were then incubated with specific primary antibodies, including mouse monoclonal anti-Ki-67 (DakoCytomation) and rabbit polyclonal anti-AR (Santa Cruz Biotechnology) at 4°C overnight in a humidity chamber. An EnVision system (DakoCytomation) was used to detect the reaction products. *In situ* detection of apoptotic cells was carried out using terminal deoxynucleotidyl transferase–mediated dUTP nick end labeling (TUNEL assay) reaction mixture according to the manufacturer's protocol (Chemicon).

Data analysis. Data are presented as the mean ± SD for the indicated number of separate experiments. The statistical significance of differences between two groups of data (Figs. 2*A* and *B*, 3*A*, and 5*A, B*, and *D*; Supplementary Fig. S1*B* and *D*; Table 1) was analyzed by paired *t* test and *P* values of <0.05 were considered significant. Dose-response curves and IC_{50} for PSA inhibition (Fig. 1*A*) and relative colony growth (Fig. 2*B*) were analyzed using a sigmoidal dose-response equation (variable slope) in Prism 3.02 (GraphPad) as described previously (9, 10).

Results

HDHS suppresses androgen-induced PSA expression. In androgen-responsive 22Rv1 cells, HDHS decreased the androgen-AR–mediated activation of PSA promoter luciferase reporter in a dose-dependent manner (Fig. 1*A*). By comparing with bicalutamide, a clinically used antiandrogen, brand name Casodex, HDHS was as potent as Casodex and achieved a complete inhibition of PSA promoter activity at concentration >10 μmol/L (Fig. 1*A*). However, the slope of the HDHS dose-response curve was steeper than that of Casodex, in which IC_{50} values of HDHS and Casodex are 4.8 and 2.5 μmol/L, respectively (Fig. 1*A*).

The AR suppression activity of HDHS was also examined in LNCaP cells, another androgen-dependent PCa cell line. Expression of endogenous PSA in treated cells as a measure of androgen response and AR activity was detected by Western blot. As shown, the intracellular expression of PSA and AR in LNCaP cells was greatly induced by DHT treatment (Fig. 1*B, lane 1* versus *2*). The AR activation of PSA expression by DHT diminished in the presence of HDHS in a concentration-dependent manner and was completely abolished by 10 μmol/L HDHS (Fig. 1*B, lanes 3–6*). The protein levels of AR in LNCaP cells were not significantly altered in cells treated with 2.5 or 5 μmol/L of HDHS but fell to basal level in cells treated with 10 μmol/L HDHS (Fig. 1*B, lane 6* versus *2*).

HDHS acts on LBD and induces AR nuclear localization. The molecular mechanism whereby HDHS represses AR activity was analyzed by the following experiments. First, a one-hybrid assay has been used to detect hormonal effects on nuclear receptors (18). Because the LBD of AR contains the AF-2 whose activation on transcription relies on binding with agonist, we transfected the AR-LBD fused with the GAL4 DNA-binding domain (GBD-AR-LBD) in 22Rv1 cells so that DHT binding to the AR-LBD can activate transcription from GAL4-response element (Fig. 1*C, left, lane 1*). Casodex competition with DHT for binding to the AR-LBD inhibited the DHT induction of AR-LBD (Fig. 1*C, left, lane 2* versus *1*). In this test, HDHS inhibited the AR-LBD dose dependently just as Casodex did (Fig. 1*C, left, lanes 3* and *4* versus *1*). Second, the AR-LBD interaction with the full-length AR can be detected by a two-hybrid interaction assay in PC-3 cells through transfection of GBD-AR-LBD and AR fused with VP16 activation domain (AR-VP16; ref. 18). Similarly to Fig. 1*C* (*left*), the two-hybrid

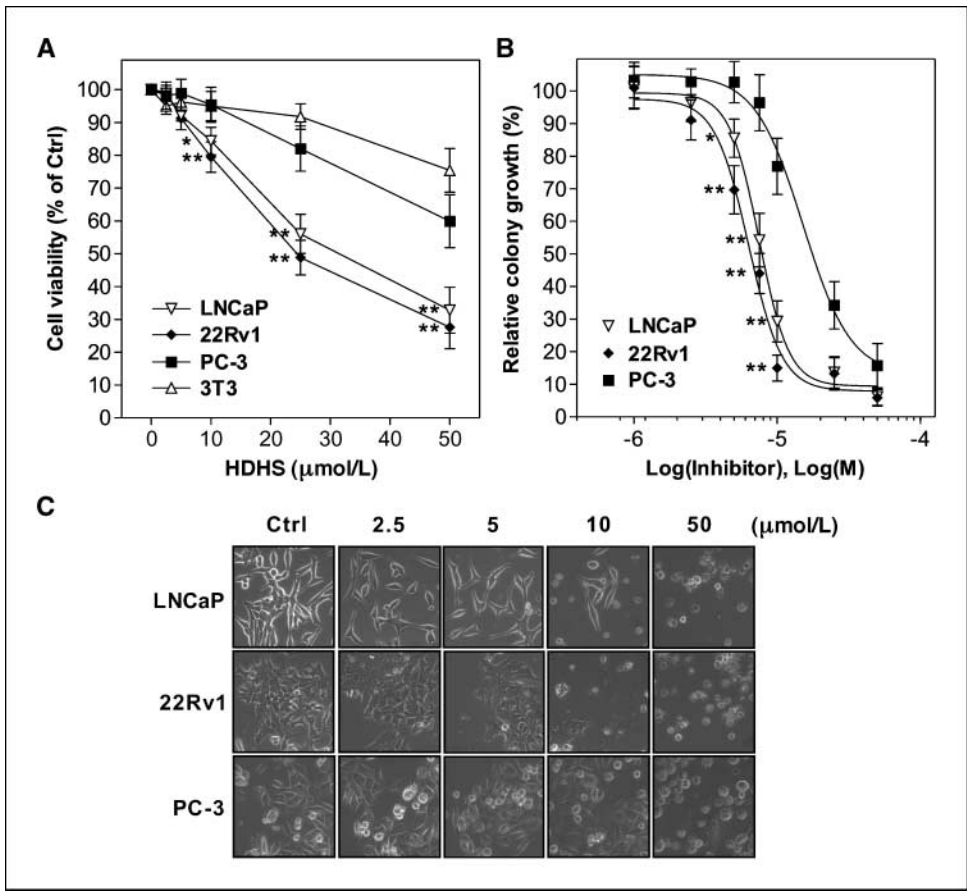

Figure 2. HDHS affects growth of PCa cells. *A,* LNCaP, 22Rv1, PC-3, and NIH-3T3 cell lines were grown and treated with vehicle (*Ctrl*) or indicated concentrations of HDHS for 48 h. Cell viability was determined by MTT assay and the absorbance of the control group was defined as 100%. *Points,* mean of three independent experiments of three replicates; *bars,* SD. *B,* colony-forming growth was analyzed by growing LNCaP and 22Rv1 cells (AR-dependent PCa cells) and PC-3 cells (AR-independent PCa cells) in 24-well multidishes with indicated treatments for 12 d. The colony-forming growth was quantified and dose-response curves were presented as percentage of growth with respect to control treatment of the same cell line. *Points,* mean of three independent experiments of three replicates; *bars,* SD. *C,* photographs of different PCa cell lines growing on culture plates with designated treatments for 2 d. AR-dependent (LNCaP and 22Rv1) and AR-independent (PC-3) cells were statistically compared. *, $P \leq 0.05$; **, $P \leq 0.01$.

interaction was stimulated by DHT and the DHT induction was competitively inhibited by Casodex and HDHS (Fig. 1*C, right*). These two tests indicate that HDHS affects the AR by blocking the action of DHT on the AR-LBD.

Third, it is known that DHT and Casodex binding to the AR will induce AR nuclear translocation (19). We examined whether HDHS treatment alone could induce AR nuclear translocation and compared this with the effects of DHT and Casodex. After steroid deprivation in LNCaP cells, AR in vehicle-treated cells was distributed in the cytoplasm and nucleus (Fig. 1*D, a*). Treatment with DHT increased the nuclear to whole-cell ratio of AR (Fig. 1*D, e*). Similarly, treatment with Casodex increased the nucleus AR ratio (Fig. 1*D, b*). Treatment with 5 to 10 μmol/L of HDHS also resulted in significant AR accumulation in the nucleus (Fig. 1*D, c* and *d*). DHT cotreatment with Casodex or HDHS also showed the same nuclear translocation of AR (Fig. 1*D, f–h*). As HDHS, such as DHT and Casodex, induces AR nuclear translocation, and as HDHS acts on the AR-LBD, this suggests that HDHS may bind to the AR-LBD as an antiandrogen.

HDHS inhibits cell growth in androgen-responsive PCa cells. Because AR is a critical growth determinant for PCa cells, the AR suppression effects of HDHS may also suppress the malignant growth of PCa cells (20–23). First, we tested the effects of HDHS on cell viability in various PCa cell lines, including androgen-dependent LNCaP, androgen-responsive 22Rv1 cells, and androgen-independent PC-3 cells, and compared them with untransformed fibroblast NIH-3T3 cells. After treating different cell lines with increasing doses of HDHS for 48 h, cell viability was determined by MTT assay, which quantitatively measures the metabolic activity of living cells. HDHS concentrations above 10 μmol/L strongly reduced cell viability in LNCaP and 22Rv1 cells but the negative effect was far less pronounced in PC-3 cells (LNCaP versus PC-3 or 22Rv1 versus PC-3) and NIH-3T3 cells (Fig. 2*A*).

Second, the long-term effect of HDHS on the malignant growth of AR-dependent (22Rv1 and LNCaP) and AR-independent (PC-3) PCa cells was examined by colony-forming growth assay. The dose-response curves of PCa cells for relative colony growth showed that 2.5 to 10 μmol/L of HDHS exerted higher antiproliferation efficacy on AR-dependent PCa cells than on AR-independent PCa cells (LNCaP versus PC-3 or 22Rv1 versus PC-3; Fig. 2*B*). The IC_{50} (antiproliferation potency) of HDHS on 22Rv1, LNCaP, and PC-3 cells was 6.3, 7.5, and 13.2 μmol/L, respectively (Fig. 2*B*). The differential effect was also reflected in the morphology of treated cells. As shown in Fig. 2*C*, LNCaP and 22Rv1 cells treated with 10 to 50 μmol/L of HDHS for 48 h exhibited cell rounding and surface blebbing, indicating apoptosis, whereas PC-3 cells treated with up to 50 μmol/L HDHS exhibited only cell rounding. All these above results suggested that HDHS possesses potent and selective toxicity toward AR-dependent PCa cells. The effect of HDHS on the cell cycle of these different cell lines was further studied by flow cytometry.

HDHS influences cell cycle progression in AR-dependent and AR-independent PCa cells differently. The effects of HDHS on the cell cycle distribution of PCa cells were examined to determine potential mechanisms of growth suppression (Table 1). After HDHS treatment for 48 h, there was a significant increase in the sub-G_1 cell population along with decreases in the G_0-G_1 and

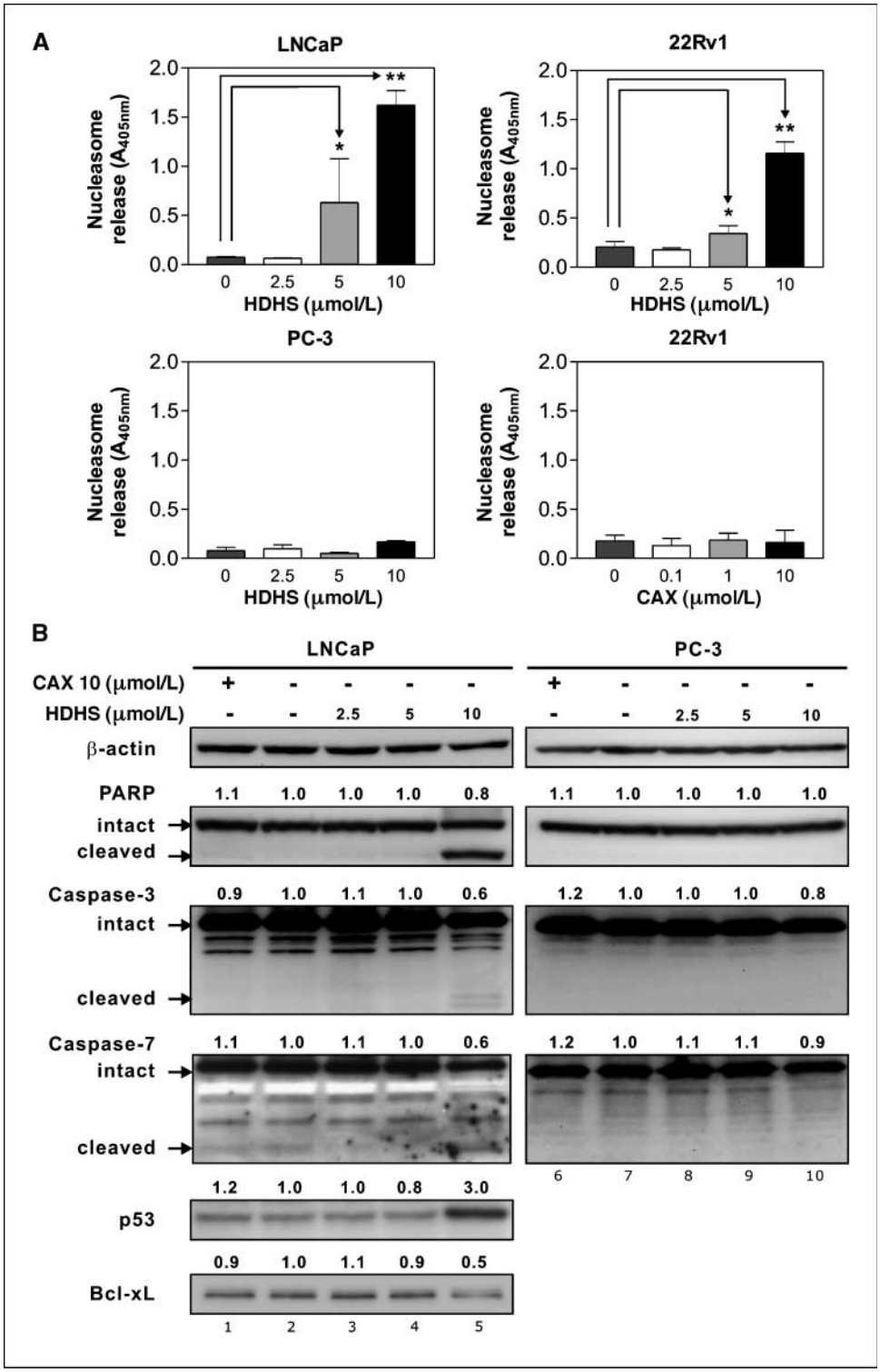

Figure 3. HDHS induces apoptosis in AR-dependent PCa cells. *A,* LNCaP, 22Rv1, and PC-3 cells (2×10^4) were treated with vehicle or indicated concentrations of HDHS for 24 h. Apoptosis of cytoplasmic DNA fragmentation was measured with Cell Death Detection ELISA Plus kit (Roche Diagnostics). *Columns,* mean of three independent experiments of three replicates; *bars,* SD. Difference between the indicated pair of treatments was tested for statistical significance as marked. *, $P \leq 0.05$; **, $P \leq 0.01$. *B,* activation of caspases and PARP in HDHS-induced apoptosis of LNCaP cells. LNCaP and PC-3 cells were grown and treated with vehicle or indicated concentrations of HDHS for 24 h. Whole-cell extracts were then subjected to Western blotting using anti-PARP, anti-caspase-3, anti-caspase-7, anti-p53, and anti-Bcl-xL antibodies. The blots represent three independent experiments.

S populations in both LNCaP and 22Rv1 cells, whereas in PC-3 cells there was an increase in the G_0-G_1 population and a decrease in the G_2-M population without any significant change in sub-G_1 populations in comparison with vehicle-treated controls. The alteration of cell cycle profiles in AR-dependent PCa cells on HDHS treatment was highly dose dependent. In LNCaP and 22Rv1 cells, the G_0-G_1 populations modestly increased with 5 μmol/L HDHS and drastically decreased with 10 μmol/L HDHS; meanwhile, the sub-G_1 populations surged. HDHS treatment for 24 h resulted in similar effects as those seen at 48 h except for a lower degree of alterations in all tested cell lines (data not shown). In contrast, treatment with 1 to 10 μmol/L of Casodex showed no appreciable change in the cell cycle distribution in any of the three PCa cell lines.

HDHS induces apoptosis in AR-expressing PCa cells. In light of the increase of sub-G_1 populations by HDHS, we further

analyzed apoptosis in treated cells via measurement of nucleosome release in PCa cells. Apoptosis was significantly induced in LNCaP and 22Rv1 cells treated with 5 to 10 μmol/L of HDHS for 24 h but not in PC-3 cells (Fig. 3*A*). 22Rv1 cells with AR expression are ablation resistant but respond to androgen stimulation; HDHS led to their apoptosis. These data also suggest that a similar mechanism may mediate the effects of HDHS on cell cycle progression in both LNCaP and 22Rv1 cells. On the other hand, treatment of 22Rv1 cells with Casodex up to 10 μmol/L for 24 h, however, failed to induce apoptosis.

During apoptosis, various caspases are activated, which are involved in the cleavage and activation of a range of critical cellular substrates, including activation of the DNA repair enzyme PARP (16, 17). In the presence of 10 μmol/L HDHS, PARP cleavage was observed, and at the same time, caspase-3 and caspase-7 were activated by proteolytic cleavage (Fig. 3*B, lane 5*). These results confirmed the flow cytometry observation that HDHS stimulates apoptosis in LNCaP cells (Table 1) and the observed nucleosome release (Fig. 3*A*). In contrast, activation of caspase-3 and caspase-7 or cleavage of PARP was not detected in PC-3 cells treated with 10 μmol/L HDHS for 24 h (Fig. 3*B, lane 10*). Tumor suppressor p53 is a critical control for the G_1 checkpoint and cell apoptosis, and LNCaP cells express wild-type p53 (24). LNCaP cells treated with 10 μmol/L HDHS for 24 h had a 3-fold increase in p53; concurrently, levels of the antiapoptotic regulator Bcl-xL decreased by ~50% (Fig. 3*B, lane 5*).

HDHS decreases expression of G_1-associated cyclins and CDKs in LNCaP and PC-3 cells. The molecular mechanisms for HDHS-induced G_0-G_1 cell cycle arrest were further assessed by the expression of the cyclins and CDKs that operate in the G_1 phase in PCa cells (12, 13). HDHS treatment of LNCaP cells for 24 h resulted in a concentration-dependent decrease in cyclins D1 and E (Fig. 4, *lanes 3–5*). Moreover, HDHS also decreased the protein levels of CDK4, CDK6, and CDK2 (Fig. 4, *lanes 3–5*). Protein expression of CDK inhibitors operative at the G_1 checkpoint, p21 and p27, also increased in the presence of 10 μmol/L HDHS (Fig. 4, *lane 5*). The HDHS-mediated down-regulation of CDKs and cyclins together suggests that CDK kinase activity and the consequent phosphorylation of Rb may decrease. Indeed, HDHS treatment markedly decreased the phosphorylation of Rb in LNCaP cells (Fig. 4, *lanes 3–5*). All the above phenomena were also observed in PC-3 cells treated with HDHS, only at a lower magnitude than in LNCaP cells (Fig. 4, *lane 10* versus *5*). As a comparison, Casodex treatment in LNCaP and PC-3 cells (Fig. 4, *lanes 1* and *6*) failed to lead to any significant change in cell cycle (Table 1). Taken together, our results indicate that HDHS induces apoptosis in AR-dependent PCa cells by arresting cell cycle at the G_1-checkpoint and activating apoptotic signaling pathways, whereas only cell cycle arrest was observed in AR-independent PCa cells on HDHS treatment.

Oral intake of HDHS suppresses growth of PCa 22v1 xenograft in nude mice. 22Rv1 cells were derived from a castration-relapsed tumor of human PCa origin that represents a

Table 1. Effect of Casodex and HDHS on cell cycle distribution in AR-dependent and AR-independent PCa cells

Treatments	G_0-G_1 phase	G_2-M phase	S phase	Sub-G_1 phase
LNCaP cells				
Control	61.7 ± 1.7	22.0 ± 1.9	11.2 ± 1.2	0.9 ± 0.5
Casodex (1 μmol/L)	62.1 ± 3.5*	21.8 ± 2.0*	10.1 ± 1.7*	1.0 ± 0.5*
Casodex (10 μmol/L)	61.3 ± 3.4*	22.3 ± 1.7*	10.4 ± 1.5*	1.3 ± 0.8*
HDHS (2.5 μmol/L)	62.6 ± 2.8*	21.1 ± 2.4*	11.5 ± 2.1*	0.8 ± 0.4*
HDHS (5 μmol/L)	66.9 ± 2.0†	18.7 ± 3.5*	8.1 ± 1.8†	3.9 ± 0.7†
HDHS (10 μmol/L)	45.1 ± 3.1‡	20.2 ± 2.1*	6.8 ± 2.4†	24.3 ± 3.1‡
22Rv1 cells				
Control	52.7 ± 2.7	25.8 ± 2.1	13.4 ± 1.5	1.4 ± 0.6
Casodex (1 μmol/L)	53.5 ± 2.6*	25.0 ± 1.6*	13.5 ± 2.3*	1.5 ± 1.1*
Casodex (10 μmol/L)	53.0 ± 3.2*	25.4 ± 1.0*	12.2 ± 1.8*	2.3 ± 1.8*
HDHS (2.5 μmol/L)	54.5 ± 2.5*	24.8 ± 2.4*	11.2 ± 1.9*	2.2 ± 0.8*
HDHS (5 μmol/L)	57.9 ± 1.9†	23.7 ± 2.7*	8.0 ± 1.4‡	3.8 ± 0.9†
HDHS (10 μmol/L)	48.4 ± 2.9‡	24.5 ± 2.0*	5.7 ± 2.2‡	14.4 ± 3.7‡
PC-3 cells				
Control	50.0 ± 2.2	26.1 ± 2.1	19.8 ± 1.6	2.0 ± 0.8
Casodex (1 μmol/L)	51.1 ± 3.6*	24.4 ± 2.5*	18.5 ± 2.1*	2.3 ± 1.5*
Casodex (10 μmol/L)	51.0 ± 2.1*	25.2 ± 2.1*	19.0 ± 1.3*	1.8 ± 1.4*
HDHS (2.5 μmol/L)	52.7 ± 2.0*	24.9 ± 2.7*	19.2 ± 1.0*	2.3 ± 0.7*
HDHS (5 μmol/L)	55.9 ± 2.9†	19.5 ± 2.9†	18.8 ± 1.1*	2.8 ± 0.9*
HDHS (10 μmol/L)	58.2 ± 2.8‡	19.2 ± 3.2†	18.0 ± 1.9*	2.1 ± 0.6*

NOTE: The cells were treated with vehicle alone or indicated dose of treatments for 48 h, stained with propidium iodide, and analyzed by flow cytometry. Percentage of cell population in sub-G_1, G_0-G_1, S, and G_2-M phases was calculated using EXPO32 ADC analysis. Each value represents the mean ± SD from two independent experiments of four replicates. Each indicated treatment versus vehicle control was statistically compared by paired *t* test.

*P = not significant.

†$P \leq 0.05$.

‡$P \leq 0.01$.

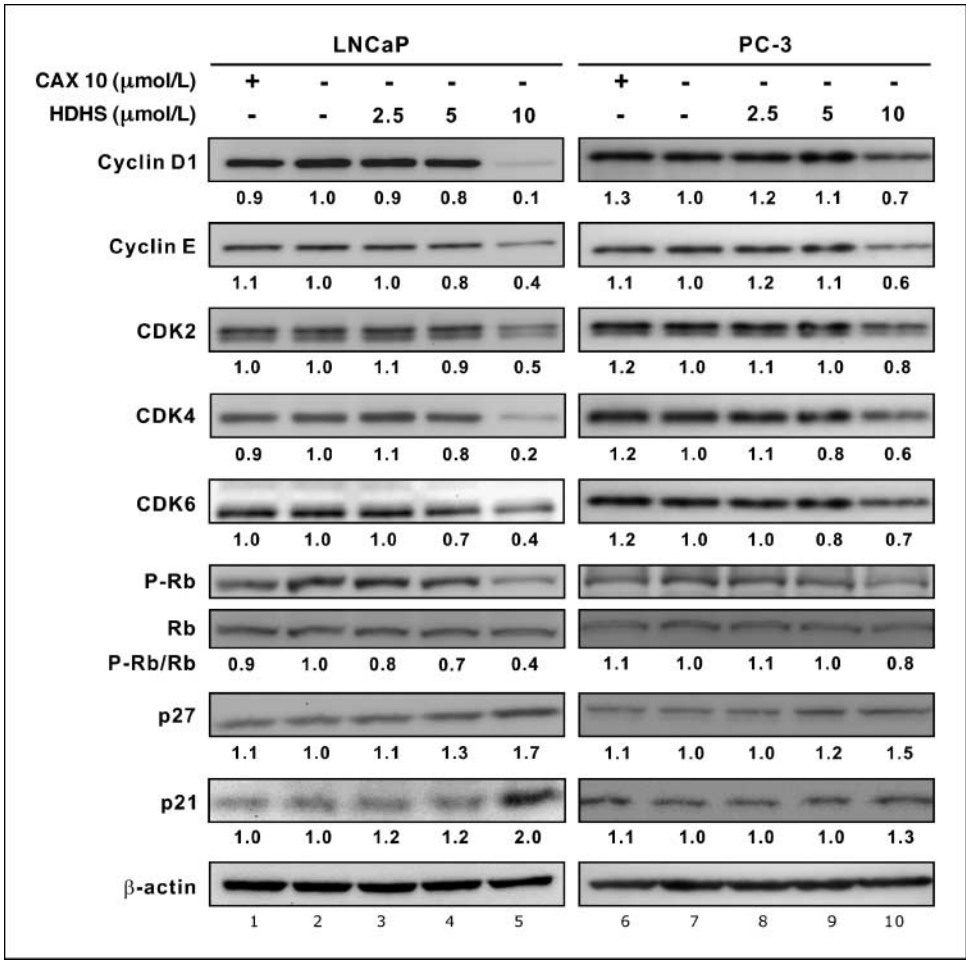

Figure 4. HDHS blocks cell cycle progression at G_1 phase and the protein expression of G_1-associated cyclins and CDKs in LNCaP and PC-3 cells. Cells were treated with indicated concentrations of HDHS or Casodex for 24 h. Cellular proteins were also harvested for the analysis of expression of cyclins D1 and E, CDK2/CDK4/CDK6, phosphorylated Rb (*P-Rb*)/Rb, p27, and p21 by Western blotting. The blots represent two independent experiments.

clinical limitation for hormonal therapy (25, 26). The potential of HDHS to withhold the growth of PCa *in vivo* was tested in athymic nude mice with a 22Rv1 tumor. Once the tumor grew to palpable size 1 week after 22Rv1 cells were implanted, HDHS was administrated by gavage once daily at doses of 0.5 and 2.5 mg/kg body weight. We measured the PCa growth according to tumor size and tumor mass at the end of HDHS treatment; both results revealed that oral intake of HDHS significantly retarded PCa growth (Fig. 5*A* and *B*). End-point tumor mass showed the dose-dependent suppression effects of HDHS (0.5 versus 2.5 mg/kg; $P \leq 0.05$; Fig. 5*B*). During the 24-day HDHS regimen, mice did not exhibit any symptoms of toxicity such as loss of appetite, decreased locomotion, or any other apparent signs of illness. As shown in Fig. 5*C*, body weight of tested mice was not influenced by HDHS at up to 2.5 mg/kg/d.

Oral intake of HDHS induces apoptosis along with a decline in cell proliferation and AR expression in PCa 22v1 xenografted nude mice. Our *in vitro* assays showed that HDHS inhibited proliferation and induced apoptosis in AR-dependent PCa cells; therefore, we went on to examine the *in vivo* effects of HDHS on proliferation and apoptosis in tumor xenografts by immunohistochemistry. Staining for proliferative tumor cells with human-specific Ki-67 antibody further revealed that oral intake of 0.5 and 2.5 mg/kg/d of HDHS for 24 days decreased the number of cells positively stained for Ki-67 (Fig. 5*D, a–c*) and resulted in an increase of apoptotic tumor cells positively stained by the TUNEL method (Fig. 5*D, d–f*). The antiproliferation and apoptosis induction effects induced by HDHS ingestion were statistically significant and the results were dose dependent (Fig. 5*D, right*). Moreover, we stained the AR expression in tumor cells, which also indicated activity of the androgen-AR axis. A prevalent decrease of AR expression was found in HDHS-treated tumors, although they remained positively stained for AR (Fig. 5*D, g–i*). This result agreed with the *in vitro* effect of HDHS (Fig. 1*B*) and suggested a debilitating activity of AR *in vivo*.

Oral intake of HDHS achieved effective concentrations in plasma and in tumors in nude mice. To further understand the dose-effect relationships, the attainable levels of HDHS in plasma and tumors were detected 24 h after the last dose of HDHS regimen in the tested mice. As shown in Supplementary Fig. S1*A* and *C*, control mice receiving vehicle only showed undetectable levels of HDHS in both plasma and tumors (chromatograms *b*), whereas HDHS ingestion resulted in sharp dose-dependent peaks in plasma and tumor levels in HPLC profiles (chromatograms *c* and *d*). Oral administration of 0.5 and 2.5 mg/kg of HDHS resulted in 0.45 ± 0.14 and 1.45 ± 0.30 μmol/L of HDHS in plasma (Supplementary Fig. S1*B*) and accumulated 98.45 ± 19.80 and 154.93 ± 12.97 nmol/g of HDHS in tumor tissues (Supplementary Fig. S1*D*). These increases of HDHS concentrations in plasma and tumors were dose dependent and coherent with the extent of tumor suppression (Fig. 5*A* and *B*).

Discussion

AR is critical for the growth and recurrence of PCa. This study shows the efficacy and potency of a new antiandrogen, HDHS, in inhibiting AR activity in PCa, which approximates that of a currently used antiandrogen. More importantly, HDHS was found to be antiproliferative and proapoptotic against an ablation-resistant 22Rv1 tumor still expressing AR and responsive to androgen. Furthermore, HDHS also inhibited PC-3 cells with a lower potency via cell cycle arrest, an AR-negative and completely androgen-independent line. There may thus be an additional unknown target with a lower affinity to HDHS in PC-3 cells. The effect of HDHS was superior to the long-used commercial antiandrogen Casodex. Data presented in this study indicate that daily ingestion of HDHS at a dose that was well tolerated over 24 days reduced the tumor growth ~40% and attained a systemic level of HDHS falling within its beneficial range. These characteristics suggest that HDHS may afford a longer period of response or a lower chance of recurrence than the current antiandrogens used in PCa treatment.

Cytotoxicity and antiproliferation tests showed that HDHS suppresses AR-dependent LNCaP and 22Rv1 cells more profoundly than AR-independent PC-3 and untransformed NIH-3T3 cells, suggesting a specific activity rather than general cytotoxicity. In addition, HDHS has low inhibitory effect on untransformed NIH-3T3 cells even in high dose range, which implies that HDHS may have less toxicity to normal cells and more advantages for clinical application. In addition to HDHS, we have taken the strategy by targeting the AR activity in 22Rv1 cells and identified four bioactive compounds in *Wedelia chinensis* and the "synergism" exerted by particular proportions in the herbal extract (9, 10). We hereby compare with HDHS the potency and efficacy of the *Wedelia* compounds and formula on antiproliferation (Supplementary Table S1).

Our cell cycle analysis provides the first evidence that HDHS promoted G_0-G_1 cell cycle arrest in PCa cells and induced apoptosis in AR-dependent cells possibly through additional mechanisms (Table 1). In AR-dependent PCa cells, G_1 arrest induced by 10 μmol/L HDHS was followed by stimulation of

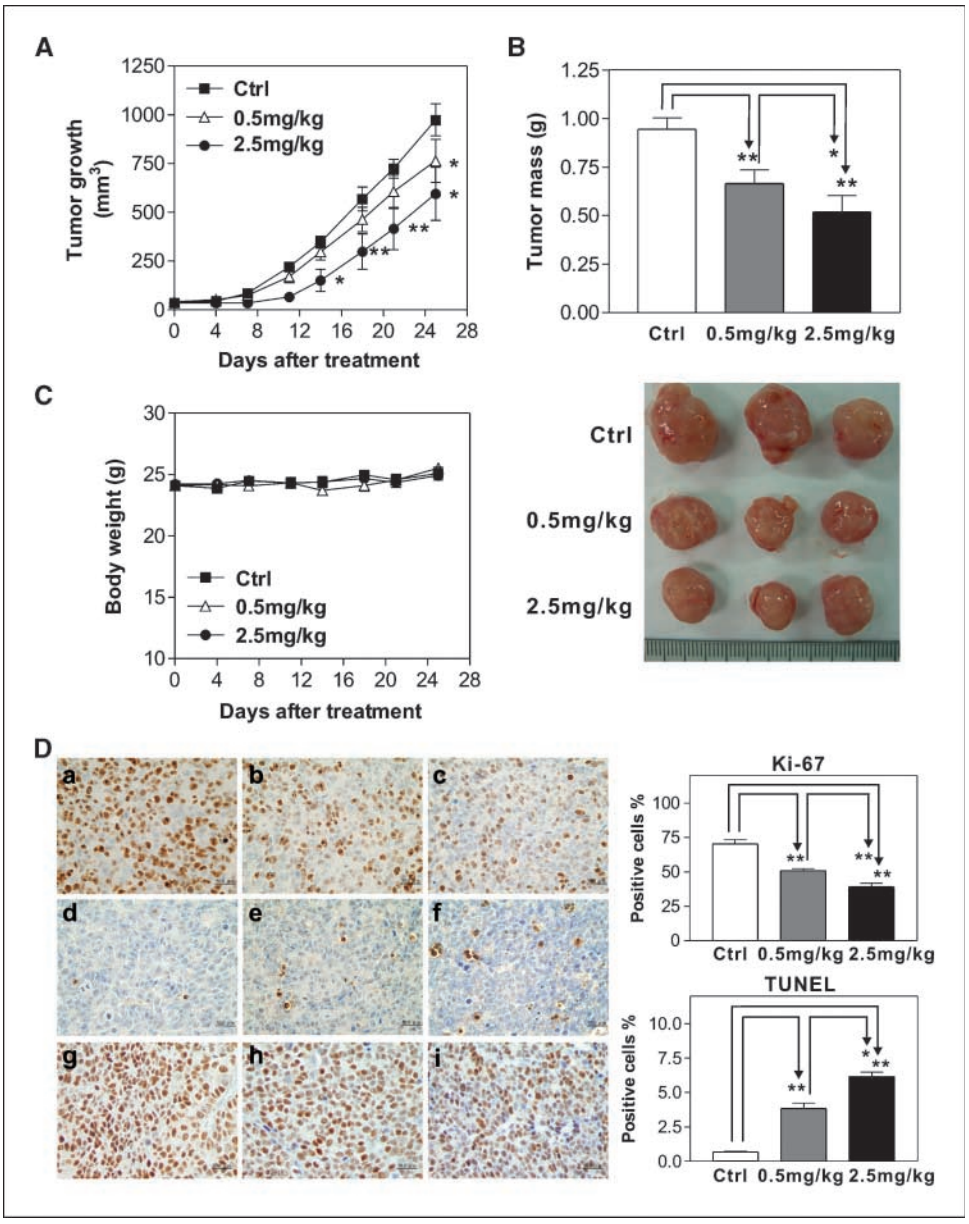

Figure 5. HDHS suppresses tumor growth of CWR22Rv1 xenograft in nude mice via inducing apoptosis and diminishing proliferation and AR expression. S.c. CWR22Rv1 tumor xenografts were established in nude mice and mice were treated with HDHS via force feeding once a day. *A,* mean tumor volume for each treatment group presented as growth curves. *Points,* mean ($n = 7$); *bars,* SE. *B,* end-point tumor mass. *Top,* tumor mass of each treatment group was statistically analyzed for significant difference as marked. *, $P \leq 0.05$; **, $P \leq 0.01$. *Bottom,* photograph of dissected tumors representing all tested groups. *C,* mean body weight for each treatment group plotted as a function of day of treatment. *D,* at the end of the xenograft study detailed in *A* to *C*, tumors were excised and processed for immunohistochemical staining for proliferation with Ki-67 (*a–c*), apoptosis by TUNEL assay (*d–f*), and AR expression (*g–i*). A representative picture of each treatment group is as shown. *Right,* Ki-67–postive and TUNEL-positive density (%) were calculated by [number of positive (reddish brown) cells × 100/total number of cells counted]. *Columns,* mean of five independent tumor samples from individual mice, of which three random areas in each tumor were counted; *bars,* SE. Each treatment group was statistically analyzed and significant differences are marked. *, $P \leq 0.05$; **, $P \leq 0.01$.

apoptosis, thereby damping the cell viability (Fig. 2*A*). In AR-independent PCa cells, 10 μmol/L HDHS arrested the cell cycle in the G_1 phase without influencing cell viability, but in the long run, the colony-forming growth was still inhibited (Fig. 2*B*).

As well as being associated with AR, the proapoptotic effects of HDHS in LNCaP cells are also associated with activation of p53; in PC-3 cells null for p53 expression, HDHS arrested the cell cycle without proapoptotic effects (24). Whether or not loss of p53 is involved in controlling HDHS-induced apoptosis needs to be further studied. Apoptosis is a programmed cell death characterized by cell shrinkage, membrane blebbing, chromatin condensation, DNA fragmentation, and selective cleavage of vital proteins by caspases (16, 17). Caspases play important roles in apoptosis triggered by various proapoptotic signals (27, 28). In HDHS-treated LNCaP cells, we observed activation of caspase-3 and caspase-7, cleavage of PARP, and down-regulation of antiapoptotic Bcl-xL protein in HDHS-treated LNCaP cells. Although the apoptotic signaling induced by HDHS remains largely unknown, the associated caspase activation and regulation of Bcl-2 family members may be involved with a permeability increase of mitochondrial outer membrane and release of cytochrome *c*, which is responsible for the activation of both caspase-7 and caspase-3.

The significance of HDHS is stressed by its efficacy at suppressing 22Rv1 xenograft tumor growth in nude mice (Fig. 5). Although many natural products exhibit potent chemopreventive activities *in vitro*, their activity against tumors *in vivo* is negligible due to their poor pharmacokinetic properties. In the cases of curcumin and the green tea epigallocatechin-3-gallate, absorption from the gastrointestinal tract is poor, even when systemically administered; the phytocompounds are quickly excreted through hepatic metabolism (29, 30). HDHS fed by gavage to mice, however, resulted in antiproliferation and apoptosis of tumor cells *in vivo* as examined by Ki-67 staining and TUNEL assay; these results agreed with the overall antitumor effects (Fig. 5). Moreover, these effects were dose dependent and positively correlated with the increase of HDHS in plasma and tumors (Supplementary Fig. S1). It is understandable that immediately after HDHS ingestion the systemic concentrations of HDHS were at a much higher level (peak effect) and remained at that level for some time (duration of action) before falling to a therapeutic margin (fluctuation). Indeed, levels as high as 98.5 ± 19.8 and 154.9 ± 12.97 nmol/g of HDHS accumulated in the tumor tissues of 0.5 and 2.5 mg/kg test groups. These concentrations were high enough to cause antiproliferation and apoptosis. The efficacy of HDHS both *in vitro* and *in vivo* is sufficient to warrant further studies to investigate the potential for HDHS in prevention and therapy of PCa.

Disclosure of Potential Conflicts of Interest

No potential conflicts of interest were disclosed.

Acknowledgments

Received 2/20/2008; revised 5/13/2008; accepted 6/10/2008.

Grant support: National Forest Bureau, Taiwan, grants 95210122001202020e145 and 962102200070202e245 (P-W. Hsiao); Academia Sinica grant 94F007 (P-W. Hsiao); and Academia Sinica postdoctoral fellow training grant (F-M. Lin).

The costs of publication of this article were defrayed in part by the payment of page charges. This article must therefore be hereby marked *advertisement* in accordance with 18 U.S.C. Section 1734 solely to indicate this fact.

We thank the Metabolomics Core Facility of Agricultural Biotechnology Research Center, Academia Sinica, for compound purification; the National Center for High-performance Computing for computer time and facilities; Dr. Sheau-Yann Shieh (Institute of BioMedical Sciences, Academia Sinica) for critical discussion; and Dr. Harry Wilson and Miranda Loney (Editorial Office, Agricultural Biotechnology Research Center, Academia Sinica) for their critical suggestions and editing the manuscript. Experiments and data analysis were performed in part through the use of the confocal microscope at the Scientific Instrument Center of Academia Sinica and with the assistance of Shu-Chen Shen.

References

1. Jemal A, Siegel R, Ward E, Murray T, Xu J, Thun MJ. Cancer statistics, 2007. CA Cancer J Clin 2007;57:43–66.
2. Crawford ED. Challenges in the management of prostate cancer. Br J Urol 1992;70 Suppl 1:33–8.
3. Pienta KJ, Smith DC. Advances in prostate cancer chemotherapy: a new era begins. CA Cancer J Clin 2005; 55:300–18; quiz 323–5.
4. Culig Z. Role of the androgen receptor axis in prostate cancer. Urology 2003;62:21–6.
5. Heinlein CA, Chang C. Androgen receptor in prostate cancer. Endocr Rev 2004;25:276–308.
6. Shah RB, Mehra R, Chinnaiyan AM, et al. Androgen-independent prostate cancer is a heterogeneous group of diseases: lessons from a rapid autopsy program. Cancer Res 2004;64:9209–16.
7. Balk SP, Ko YJ, Bubley GJ. Biology of prostate-specific antigen. J Clin Oncol 2003;21:383–91.
8. Cleutjens KB, van der Korput HA, van Eekelen CC, van Rooij HC, Faber PW, Trapman J. An androgen response element in a far upstream enhancer region is essential for high, androgen-regulated activity of the prostate-specific antigen promoter. Mol Endocrinol 1997;11:148–61.
9. Lin FM, Chen LR, Lin EH, et al. Compounds from *Wedelia chinensis* synergistically suppress androgen activity and growth in prostate cancer cells. Carcinogenesis 2007;28:2521–9.
10. Tu WC, Wang SY, Chien SC, et al. Diterpenes from *Cryptomeria japonica* inhibit androgen receptor transcriptional activity in prostate cancer cells. Planta Med 2007;73:1407–9.
11. Evan GI, Vousden KH. Proliferation, cell cycle and apoptosis in cancer. Nature 2001;411:342–8.
12. Malumbres M, Barbacid M. To cycle or not to cycle: a critical decision in cancer. Nat Rev Cancer 2001;1: 222–31.
13. Massague J. G1 cell-cycle control and cancer. Nature 2004;432:298–306.
14. Oswald F, Dobner T, Lipp M. The E2F transcription factor activates a replication-dependent human H2A gene in early S phase of the cell cycle. Mol Cell Biol 1996; 16:1889–95.
15. Braithwaite AW, Sturzbecher HW, Addison C, Palmer C, Rudge K, Jenkins JR. Mouse p53 inhibits SV40 origin-dependent DNA replication. Nature 1987;329:458–60.
16. Herceg Z, Wang ZQ. Failure of poly(ADP-ribose) polymerase cleavage by caspases leads to induction of necrosis and enhanced apoptosis. Mol Cell Biol 1999;19: 5124–33.
17. Okada H, Mak TW. Pathways of apoptotic and non-apoptotic death in tumour cells. Nat Rev Cancer 2004;4: 592–603.
18. Hsiao PW, Chang C. Isolation and characterization of ARA160 as the first androgen receptor N-terminal-associated coactivator in human prostate cells. J Biol Chem 1999;274:22373–9.
19. Masiello D, Cheng S, Bubley GJ, Lu ML, Balk SP. Bicalutamide functions as an androgen receptor antagonist by assembly of a transcriptionally inactive receptor. J Biol Chem 2002;277:26321–6.
20. Isaacs JT, Isaacs WB. Androgen receptor outwits prostate cancer drugs. Nat Med 2004;10:26–7.
21. Scher HI, Buchanan G, Gerald W, Butler LM, Tilley WD. Targeting the androgen receptor: improving outcomes for castration-resistant prostate cancer. Endocr Relat Cancer 2004;11:459–76.
22. Scher HI, Sawyers CL. Biology of progressive, castration-resistant prostate cancer: directed therapies targeting the androgen-receptor signaling axis. J Clin Oncol 2005;23:8253–61.
23. Zou JX, Zhong Z, Shi XB, et al. ACTR/AIB1/SRC-3 and androgen receptor control prostate cancer cell proliferation and tumor growth through direct control of cell cycle genes. Prostate 2006;66:1474–86.
24. van Bokhoven A, Varella-Garcia M, Korch C, et al. Molecular characterization of human prostate carcinoma cell lines. Prostate 2003;57:205–25.
25. Nagabhushan M, Miller CM, Pretlow TP, et al. CWR22: the first human prostate cancer xenograft with strongly androgen-dependent and relapsed strains both *in vivo* and in soft agar. Cancer Res 1996;56:3042–6.
26. Sramkoski RM, Pretlow TG II, Giaconia JM, et al. A new human prostate carcinoma cell line, 22Rv1. In Vitro Cell Dev Biol Anim 1999;35:403–9.
27. Nunez G, Benedict MA, Hu Y, Inohara N. Caspases: the proteases of the apoptotic pathway. Oncogene 1998; 17:3237–45.
28. Thornberry NA, Lazebnik Y. Caspases: enemies within. Science 1998;281:1312–6.
29. Landis-Piwowar KR, Huo C, Chen D, et al. A novel prodrug of the green tea polyphenol (−)-epigallocatechin-3-gallate as a potential anticancer agent. Cancer Res 2007;67:4303–10.
30. Sharma RA, Steward WP, Gescher AJ. Pharmacokinetics and pharmacodynamics of curcumin. Adv Exp Med Biol 2007;595:453–70.

A Novel Diterpene Suppresses CWR22Rv1 Tumor Growth *In vivo* through Antiproliferation and Proapoptosis

Feng-Min Lin, Chin-Hsien Tsai, Yu-Chih Yang, et al.

Cancer Res 2008;68:6634-6642.